Physio-chemical characterization of three components co-amorphous systems generated by a melt quench method

A. D'Angelo[1], B. Edgar [1], A.P. Hurt[1], M.D. Antonijević [1]

[1] Faculty of Engineering and Science, University of Greenwich, Chatham Maritime, ME4 4TB, UK

Corresponding author M.D. Antonijevic:

- Mail: M.Antonijevic@greenwich.ac.uk
- Tel: +442083319841
- Fax: +442083319805
- Address: Faculty of Engineering and Science, University of Greenwich, Chatham Maritime, ME4 4TB, UK
- ORCID number: https://orcid.org/0000-0002-5847-7886

ABSTRACT

The purpose of this work was to evaluate the possibility of creating a ternary co-amorphous system and to determine how the properties of a co-amorphous material are altered by the addition of a selected third component. Piroxicam and indomethacin form a stable co-amorphous with the *Tg* above room temperature. The third component added was selected based on tendency to crystallise (benzamide, caffeine) or form amorphous (acetaminophen, clotrimazole) on cooling. Generated co-amorphous systems were characterised with TGA, HSM, DSC, FTIR, and XRD.

Stable ternary co-amorphous systems were successfully generated, which was confirmed using XRD, DSC and FTIR analysis. In all cases, *Tg* of the ternary system was lower than the *Tg* of the binary system, although higher than that of the individual third compound. Upon storage for 4 weeks all created ternary systems showed significantly smaller variation in *Tg* compared to the binary system.

Stable three-component co-amorphous systems can be generated via melt quench method using either a crystalline or amorphous third component. Addition of third component can alter the *Tg* of co-amorphous system and in all cases created more stable co-amorphous system upon storage. Physical parameters may not be sufficient in predicting the resulting *Tg*, therefore knowledge of chemical interaction must be brought into equation as well.

KEYWORDS: CO-AMORPHOUS – STABILITY – *Tg* – CRYSTALLINITY - AMORPHICITY

LIST OF ABBREVIATIONS

AC	Acetaminophen
API	Active Pharmaceutical Ingredient
ATR-FTIR	Attenuated Total Reflectance Fourier Transform-Infra Red Spectroscopy
BZD	Benzamide
CAF	Caffeine
CTMZ	Clotrimazole
DSC	Differential Scanning Calorimetry
HSM	Hot-Stage Microscopy
IND	Indomethacin
NCE	New Chemical Entity
PXC	Piroxicam
Tc	Crystallisation Temperature
Tg	Glass-Transition Temperature
TGA	Thermo-Gravimetric Analysis
Tm	Melting Temperature
XRD	X-Ray Diffraction

INTRODUCTION

Approximately 90 % of new chemical entities (NCE) and 40 % of drugs on the market are poorly water soluble [1] [2]. Low solubility drugs are characterised by slow dissolution rates and slow drug adsorption which leads to inadequate bioavailability and gastrointestinal toxicity [3]. Therefore, solubility improvement is a critical challenge in drug development.

Alteration of the solid state of a drug from crystalline to amorphous form offers improved apparent solubility and dissolution that leads to an increase in bioavailability [4]. Amorphous materials are characterised by short-range structural order, lacking the long-range order that instead is typical of crystalline solids. They retain an excess of enthalpy, entropy and Gibbs free energy, which is responsible for the improved apparent solubility and dissolution rate. As energy is released from the system amorphous materials convert into their crystalline counterpart, by doing so the properties of the materials inevitably change [5] [6] [7].

Amorphous materials are often produced by a quench-cooling method where samples are melted and rapidly cooled so that molecular conformation of the liquid material is preserved into the solid. Amorphous materials can also be generated by introduction of energy in the system by energetic grinding or by fast solvent removal. Different preparation methods may induce different molecular organisation. Therefore, properties of the generated amorphous material might vary [8].

As the kinetic interactions between the polymer and the amorphous active ingredient improve dissolution rate, bio-performance and stability, amorphous active ingredients are preferably delivered as polymeric solid dispersions. [9]. However, miscibility of the active ingredient in the polymer is one of the major issues in amorphous solid dispersions [10] [11] [12] . To overcome poor miscibility issues the amount of polymer is increased, this causes volume enlargement of the dosage form [13] [14]. Furthermore, amorphous materials are more hygroscopic than crystalline materials and the glass-transition temperature of most amorphous drugs is lowered, even with only a very small water content [15][16] [17] [18]. Therefore, the phase change of an amorphous active ingredient dispersed in a polymer is facilitated by the hygroscopic nature of the polymer adopted, which has caused the recall of many products by the FDA [1].

An amorphous dispersion of low molecular weight ingredients is defined as a co-amorphous mixture [19]. Co-amorphous drug delivery systems have recently attracted the interest in the pharmaceutical field to overcome limitations of solid dispersions, improve bioavailability and stability of the single amorphous components [20].

A co-amorphous is frequently composed by two low molecular weight co-formers and primarily identified by a single glass-transition temperature (*Tg*), indicating that the components are miscible and are interacting. Low molecular weight co-formers as amino acids and saccharides have shown to stabilise amorphous poorly soluble drugs by generation of co-amorphous systems [21] [22]. Active ingredients are also used as low molecular weight co-formers with the advantage of the co-administration of therapeutics. The first example presented in literature was proposed by Yamamura et al. [23] where a stable co-amorphous of cimetidine and indomethacin was generated by solvent evaporation method. Since then multiple co-amorphous systems composed by two active ingredients have been studied.

This work aims to investigate whether a three component co-amorphous system can be created reliably using a melt quench method as way to stabilise amorphous materials by improvement of their singular glass transitions and stability upon storage. The delivery of three components co-amorphous systems would have the advantage of allowing the simultaneous administration of APIs, to reduce the number of medications consumed by the patient and therefore improve patient compliance. Multi-components coamorphous systems could be used to combine the administration of two APIs that act in synergy and a chemical ingredient that facilitates their absorbance, as for example the caffeine.

Among the selected active crystalline ingredients majority were characterised by poor solubility in water (Table 1). The generation of multiple components co-amorphous system aimed to improve the apparent solubility and dissolution rate of the co-amorphous constituents. In the pharmaceutical field, there is a great interest in the systematic knowledge of the influence of the third component as it is not jet defined.

Table 1. Solubility in water of selected ingredients based on data collected in PubChem database [24]

Chemicals	Solubility in water/mg ml^{-1}	Solubility description based on Pharmacopoeia definitions
PXC	0.9370	Sparingly soluble
IND	23.0000	Sparingly soluble
BZD	0.0182	Slightly soluble
CAF	2.16×10^4	Freely soluble
AC	0.0227	Slightly soluble
CTMZ	29.8400	Sparingly soluble

MATERIALS AND METHODS

Materials were chosen from initial preliminary test where different APIs were analysed using differential scanning calorimetry (DSC) to determine their propensity to form amorphous or crystalline materials upon cooling from a melt with different cooling rates.

Piroxicam (PXC) (Sigma Aldrich, Lot: SLBG9097V) and indomethacin (IND) **(**Tokyo Chemical Industry, Lot: JU2BN-AB) were selected due to the formation of stable amorphous state with glass transition temperatures above room temperature.

The third components added to the binary combination of PXC and IND were chosen from the API screening previously described. Benzamide (BZD) (Sigma Aldrich, Lot: STBF1753V) and caffeine (CAF) (Sigma Aldrich, Lot: S21606-124) were selected due to their strong tendency to crystallise on even when melted material was subjected to Newtonian cooling. Acetaminophen (Sigma Aldrich, Lot: SLBH0185V) and clotrimazole (Tokyo Chemical Industry, Lot: PCZNB-QA) were chosen as they showed a propensity towards forming an amorphous on cooling. Physical mixtures were prepared in 1:1:1 molar ratio.

The production of amorphous samples was conducted by melting and rapidly cooling within the differential scanning calorimetry (DSC) instrument as rapid cooling of the melted sample is one of the many validated techniques used to generate an amorphous from a crystalline material [25]. Before analysis, all samples were finely ground using an agate mortar and pestle to ensure a homogenous distribution of components and to reduce the possibility of thermal lag within larger particles.

Physical mixtures and melt-cooled products were characterised with Thermo-gravimetric analysis (TGA), Hot-stage microscopy (HSM), DSC, X-ray diffraction (XRD) and attenuated total reflection Fourier transformer-Infra Red spectroscopy (ATR-FTIR). Physical mixtures were analysed to verify that simple grinding did not altered the solid state of the sample, whiles the analysis of the products assured the adopted preparation method induced complete amorphisation of the mixture components.

TGA was conducted using the Q5000 IR TGA (TA Instruments, UK) in aluminium pans with sample size 2.0 ± 0.5 mg. Samples were heated from ambient temperature (20°C) to 300°C at 10°C min^{-1}, under nitrogen (25

ml/min). HSM was conducted using a Mettler Toledo FP90 Central processor with a FP82HT Hot Stage. The heating program used was 10°C min^{-1} from 30°C to 300°C. This allowed the visual identification of thermal events (melting, crystallisation, evaporation and degradation). This data was combined with that gathered from TGA to determine the maximum temperature for the DSC experiments. DSC was carried out using a Q2000 DSC (TA Instruments, UK) in hermetically sealed Tzero aluminium pans with 2.0 ± 0.5 mg of sample. Heating rates were kept consistent throughout experiments to ensure comparable data however, the end temperature of experiments were different for each mixture. Three heating and cooling cycles were conducted for the samples to assure the homogeneity of the products and to evaluate possible differences in *Tg* measured in each heating cycle. Experiments were conducted in triplicate under Nitrogen atmosphere (flow rate 50 ml min^{-1}). Data was analysed using TA Advantage Universal Analysis V5.5.22 software. Co-amorphous systems were produced in situ using the capability of the DSC to control heating and cooling rate, then used to characterise the thermal transitions of the products.

Samples were equilibrated at -80°C then heated to 180°C with 10°C min^{-1} heating rate to erase the solid history of the samples and ensure mixing of the component molecules to form a homogeneous dispersion. After melting, the samples were cooled. To analyse the propensity of the materials to convert into amorphous, crystalline or a mixture of the phases, two different cooling rates were selected: a fast cooling rate of 20°C min^{-1} and a slow cooling rate of 5°C min^{-1} were chosen. All physical mixtures were heated to analyse the generated co-amorphous. Experiments were conducted using multiple heating and cooling cycles to determine the reproducibility of the thermal events over repeated cycles. During the final cooling ramp, the samples were brought to 20°C and subsequently stored in a temperature-controlled room at 20°C. Experiments were conducted in triplicate to verify the reproducibility of the obtained results.

XRD was conducted using a D8 Advance X-ray Diffractometer (Bruker, Germany) with theta-theta geometry in reflection mode. Cu Kα radiation at 40 kV and 40 mA was used to irradiate samples from a 0.2 mm exit slit. Data collection was between 2-40° 2θ, step size of 0.02° and a counting time of 0.3 seconds per step. Data collected was done using DIFFRAC plus XRD Commander Version 2.6.1 software (Bruker-AXS), qualitative assessment with the aid of EVA version 16.0 (Bruker-AXS). The spectrum two FT-IR spectrophotometer (PerkinElmer, UK) fitted with the Diamond/ZnSe ATR (Single Reflection) accessory was used. 16 scans were collected over the range of 4000-650 cm^{-1}. Data was analysed using the Spectrum 10™ software suite.

The initial stability study was conducted under laboratory conditions over period of one month to assess whether generated co-amorphous system will remain intact, without exposure to any exaggerated conditions. Samples were stored in sealed glass containers at 20°C away from excessive vibration and sunlight. They were tested every 7 days using DSC to analyse changes in transitions and therefore the solid state of the systems.

RESULTS AND DISCUSSION

DIFFERENTIAL SCANNING CALORIMETRY

DSC traces (Figure 1) showed that indomethacin converts into an amorphous upon rapid cooling (20°C min^{-1}) with a *Tg* of 47.9°C, which is stable upon heating. The PXC subjected to the same conditions formed an amorphous with a *Tg* of 64.6°C which recrystallizes on reheating at the temperature of 138.1°C, then melts at 181.4°C. This also shows the polymorphism exhibited by piroxicam [26]. Thermal transitions of other staring materials are shown in Table 2.

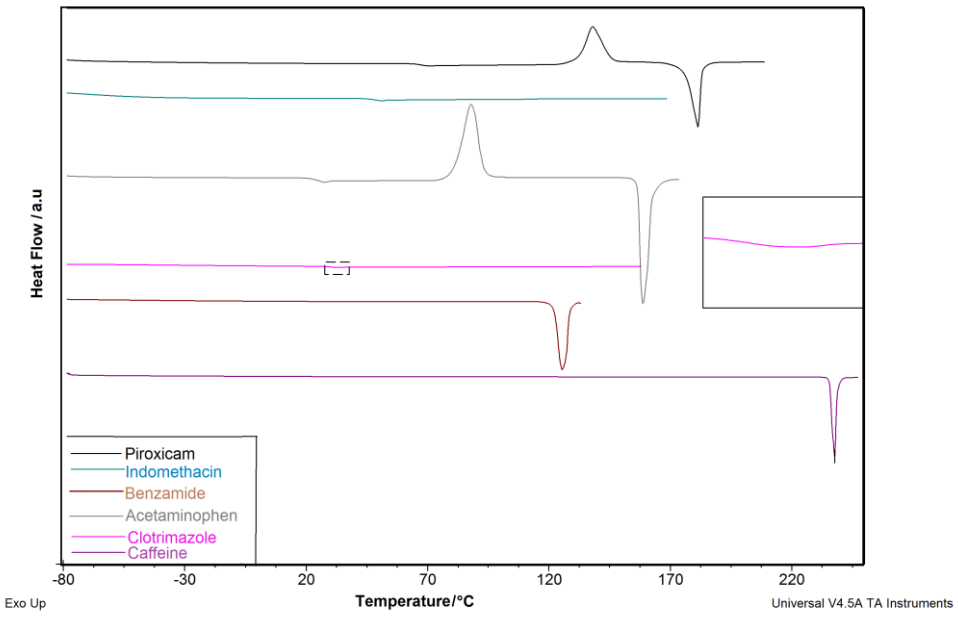

Figure 1 DSC overlay of the pure chemicals under screening, traces presented are the relative to the second heating cycle subsequent a fast cooling of the melted material.

Table 2. Thermal event measured in DSC traces of pure compounds (*n=3*)

Chemicals	Melting point on initial heating/°C	Crystallization on cooling/°C	Thermal events on 2nd heating/°C		
			Tg	***Tc***	***Tm***
PXC	203.1 ± 0.1	-	64.6 ± 1.0	138.1 ± 0.9	181.4 ± 0.6
IND	161.1 ± 0.1	-	47.9 ± 0.7	-	-
BZD	126.2 ± 0.3	98.5 ± 0.7	-	-	125.5 ± 0.1
CAF	236.7 ± 0.1	232.1 ± 0.6	-	-	237.7 ± 0.1
AC	169.8 ± 0.2	-	24.9 ± 0.6	87.9 ± 0.4	158.6 ± 0.7
CTMZ	145.5 ± 0.1	-	30.1 ± 0.3	-	-

[a] *Tg* – Glass transition, *Tc* – Crystallisation, *Tm* – Melting.

The physical mixture composed of PXC and IND at a 1:1 molar ratio was analysed in the DSC, the sample was heated above the melting of both constituents, cooled at 20°C min^{-1} and reheated to characterise the generated product.

The DSC trace of the heating cycle after subsequent cooling revealed a single *Tg* at 57.6°C which was stable upon cooling, as no recrystallization occurred, and no re-crystallisation was present on heating. This was an indication of the generation of a co-amorphous system comprising PXC and IND characterised by a *Tg* intermediate between the *Tg*s of the single components. Hence, the amorphous IND was stabilised by the interaction with the amorphous PXC as obtained *Tg* is greater than *Tg* of IND. The IND is in turn stabilising the amorphous PXC and preventing it from crystallising on reheating.

Third components were added to the binary mixture of IND and PXC, these were characterised in DSC as in Table 1, physical mixtures were in 1:1:1 molar ratios. Co-amorphous systems were produced in situ using the capability of the DSC to control heating and cooling rate, then used to characterise the thermal transitions of the products.

The physical mixture of PXC-IND-BZD cooled at 20°C min^{-1} had only a single *Tg* in the second heating cycle at 31.0°C, therefore these characteristics were associated to a co-amorphous system, which was further analysed. The BZD as pure compound showed a strong propensity to form crystalline material upon quench cooling giving such an exothermic response that the signal became a loop instead of a peak as the temperature of the cell was increased. Because of the strong propensity of the BZD to recrystallise, the generated ternary mixture had a *Tg* lower than the glass transitions of the other components.

DSC traces of the mixture with CAF presented no crystallisation upon cooling indicating the generation of an amorphous material and a single *Tg* at 45.8°C, which re-crystallised at 106.6°C and then melted at 131.3°C. These two events can be shown to be of very close enthalpies, which indicates it is a single crystal phase (one polymorph) crystallising from the mixture and then melting again. This also shows that the initially created material was entirely amorphous. The melting point of the re-crystallised material was compared with the melting temperatures of the single pure components of the system and of their polymorphic forms. However, this comparison was not sufficient to identify the entity that undergoes recrystallization.

Both CAF and BZD, although as pure compounds presented the propensity to generate crystalline materials upon heating after cooling of the melted compound, are shown to generate stable co-amorphous ternary systems in association with PXC and IND. The *Tg* of the co-amorphous system containing CAF was significantly higher than the Tg of the co-amorphous incorporating BZD. This is likely related to the elevated *Mp* of the CAF, in comparison to BZD, and therefore to the strong interactions existing between the molecules of CAF.

The amorphous form of pure AC has the lowest glass transition of all the examined compounds; however, the glass transition of this co-amorphous is dramatically higher than the glass transition of the pure AC, showing the potential of this approach to stabilising low Tg materials. The CTMZ was characterised by a low *Tg* at 30.1°C, significantly lower than the glass transitions of the pure IND and PXC; however, the co-amorphous generated by the melting of this three-component mixture had a Tg at 53.3°C, very similar with the glass transition of the binary system. The ternary system has therefore stabilised the amorphous CTMZ without altering the stability of the PXC-IND co-amorphous system.

The formulations described above were also analysed with a cooling rate of 5°C min^{-1} cooling. From Table 3 it is possible to observe the difference in glass transition measured for ternary co-amorphous from the heating cycle after cooling rate of 20°C min^{-1} and 5°C min^{-1} is smaller than the difference in Tg values encountered for the binary system. It is important to notice that the cooling rate has not influenced the PXC IND CAF system, which crystallises upon heating and then melts at the same temperature obtained from DSC traces of the heating following the fast cooling.

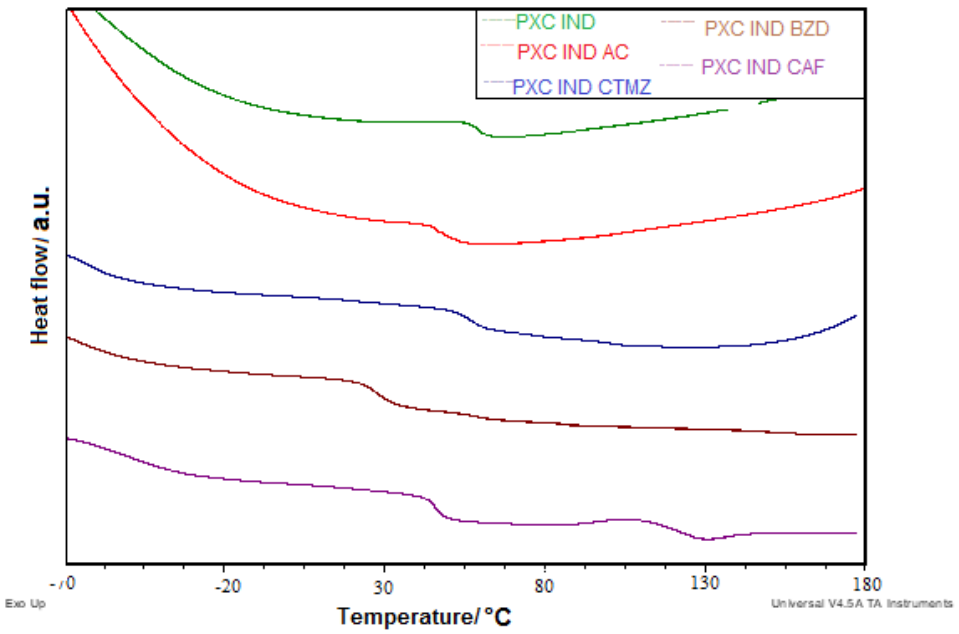

Figure 2 DSC overlay of pure binary and ternary mixtures under screening, traces presented are the relative to the second heating cycle subsequent a fast cooling of the melted material

Table 3. Thermal events measured from heating cycle subsequent cooling with cooling rates of 20°C min^{-1} and 5°C min^{-1} (*n=3*)

Chemicals	**Thermal events on heating after 20°C min^{-1} cooling/°C**			**Thermal events on heating after 5°C min^{-1} cooling/°C**			**Δ*Tg* between adopted cooling rates/C**
	Tg	***Tc***	***Tm***	***Tg***	***Tc***	***Tm***	
PXC-IND	57.6 ± 0.4	-	-	52.5 ± 0.2	-	-	5.1
PXC-IND-BZD	31.0 ± 1.2	-	-	28.8 ± 1.3	-	-	2.2
PXC-IND-CAF	45.8 ± 0.5	106.6 ± 0.4	131.3 ± 0.4	44.5 ± 1.5	106.6 ± 0.4	131.3 ± 0.4	1.3
PXC-IND-AC	47.1 ± 1.3	-	-	46.1 ± 2.1	-	-	1.0
PXC-IND-CTMZ	53.3 ± 1.2	-	-	53.5 ± 3.3	-	-	-0.2

[a] *Tg* – Glass transition, *Tc* – Crystallisation, *Tm* – Melting.

Repeatability was tested by exposing every sample to consecutive heating and cooling cycles. In these experiments, heating and cooling rates were not modified but were cycled multiple times. The standard deviation between the glass transition temperatures of the PXC IND was 0.4°C when evaluated in heating cycles after fast cooling, and 0.2°C in slow cooling experiments. Whereas ternary mixtures revealed higher variations in Tg measured in fast and slow cooling experiments (Table 3). This points out to the importance of careful selection of appropriate cooling rate in order to obtain reproducible quality of co-amorphous system.

Hot Stage Microscopy

Each physical mixture was subjected to repeated heating and cooling cycles with the same ramp rate and temperature limits as used in the DSC analysis. HSM video revealed the same thermal transitions identified in the DSC traces confirming those results. Additional information was gathered from the HSM video of the PXC IND BZD system (Fig. 3). The video collected from the heating of the co-amorphous system confirmed a glass transition, which started at 47.3°C (Fig. 3-B) and finished at 92.4°C (Fig. 3-C). However, unlike the DSC data, HSM showed evidence of the generation of crystalline material at 100.0°C, with defined needle-like shape, emerging from the rubbery material (Fig. 3-D). These crystals were not homogenously distributed in the melted sample and grew reaching maximum dimensions at 148.3°C (Fig. X-E), melting was observed in a range from 152.6°C to 160.8°C (Fig. 3-F and G).

The melting temperature of the newly generated crystals was compared with the melting temperature of the pure components of the system and possible polymorphic forms, but it was not possible identify the component that recrystallised. PXC IND BZD was the only generated co-amorphous that presented this peculiar recrystallisation behaviour where the DSC did not show the thermal event. This suggests the possibility of concurrently processes producing a net zero heat flow or that the energy released during recrystallisation is low causing the DSC to show no signal for the event. However, the recrystallisation observed in the HSM might be initiated by the energy introduced in the sample when scrapped from the DSC pan.

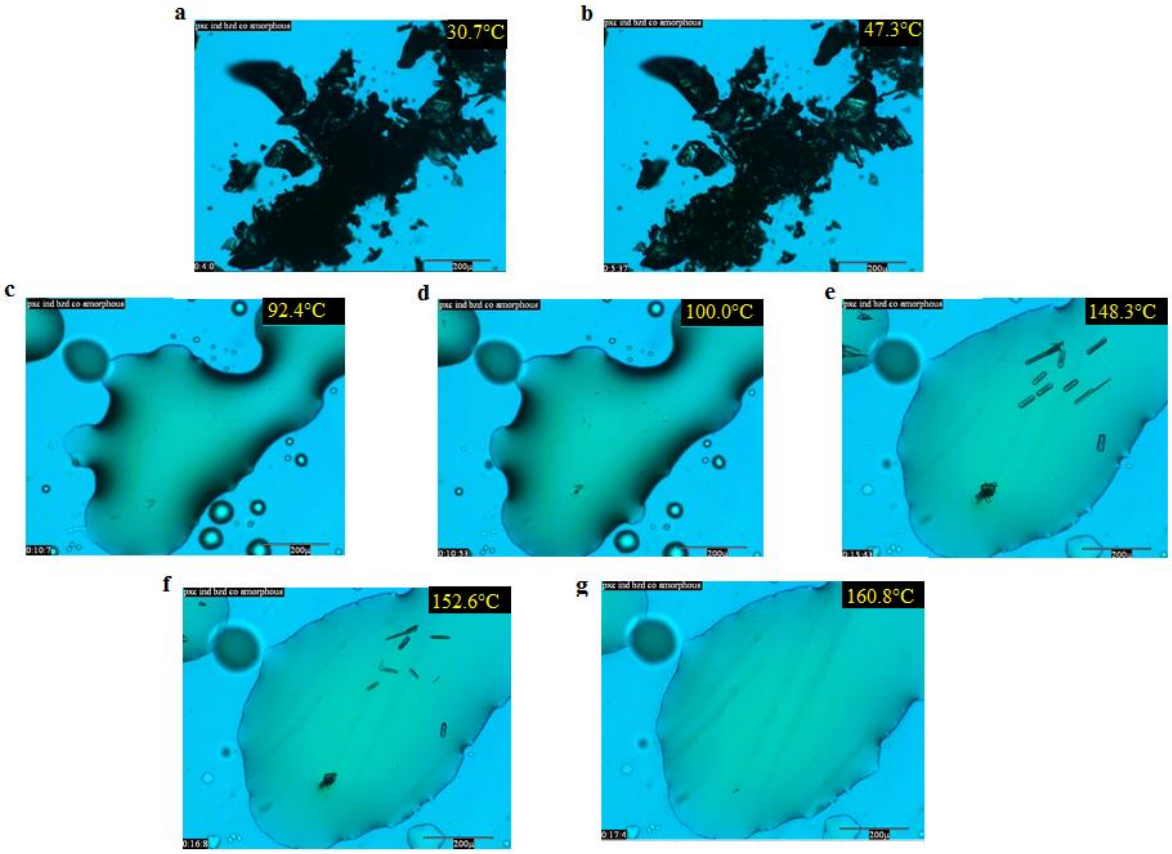

Figure 3 Images extracted from the heating process of PXC-IND-BZD realised under HSM. Each section describes as follow: **a)** the structure of the examined particle at the starting temperature; **b)** the initial stages of the glass transition (47.3^{0}C); **c)** generated rubbery amorphous (92.4^{0}C); **d)** appearance of the first crystals from the rubbery amorphous (100^{0}C); **e)** crystal growth (148.3^{0}C); **f)** melting of crystals generated (152.6^{0}C); **g)** final stage of melting (160.8^{0}C).

To further characterise the PXC IND BZD co-amorphous, a fresh sample was heated up the temperature where the initial traces of the crystals were visible (100°C) and left isothermal for one hour. A similar process was carried out for the PXC IND CAF co-amorphous, which has shown recrystallisation of a material upon heating of the created co-amorphous. This sample showed homogeneous recrystallisation upon heating at 83°C, therefore the sample was heated at 10°C min^{-1} up to 83°C and then left isothermal for one hour.

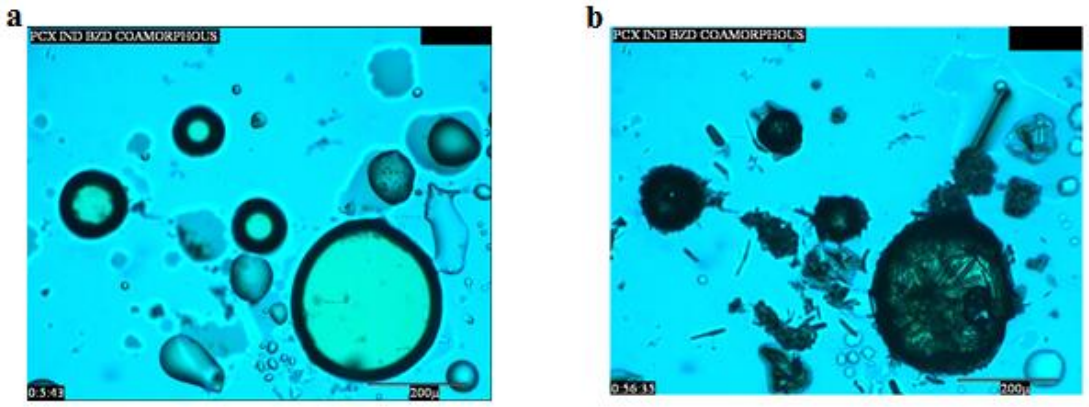

Figure 4 Images of PXC-IND-BZD co-amorphous subjected to heating above melting up to 100^0C when crystallisation starts **(a)** and left isothermal for 1 hour **(b)** to allow crystal growth.

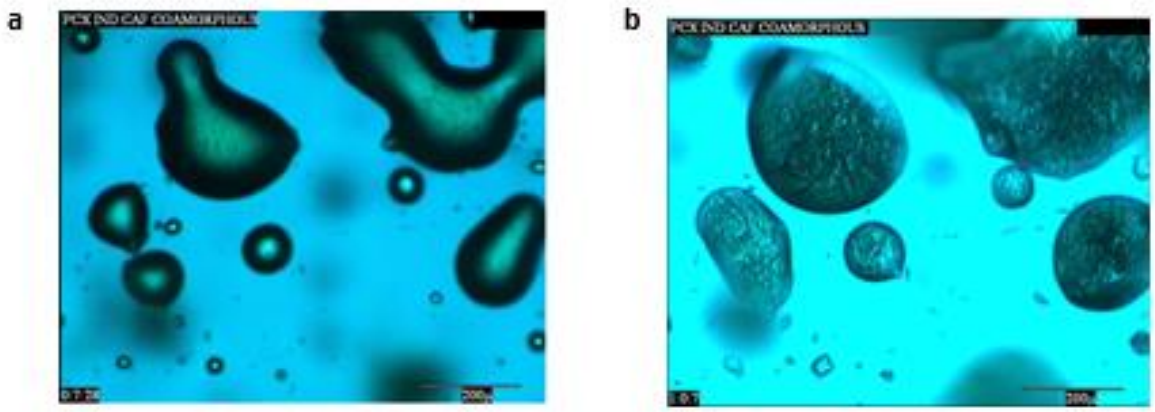

Figure 5 Images of PXC-IND-CAF co-amorphous subjected to heating above melting up to 83^0C when crystallisation starts (**a**) and left isothermal for 1 hour (**b**) to allow crystal growth.

Both samples showed a clear increase in crystal dimensions over the isothermal period. In the PXC-IND-BZD co-amorphous, crystals were formed initially in the borders of the rubbery material and in localised nucleation centres. Crystal growth was quantified from the video measuring length of the selected crystals with the HSM software at specified time intervals. The growth of the crystals was analysed up to the moment where the crystal encountered others making difficult to quantify the length. Results showed an initial elevated length increase starting at 0.07 µm sec^{-1} after only 30 seconds, decreasing to 0.03 µm sec^{-1} after 90 seconds of isothermal. Interestingly, the growth was stable at 0.04 µm sec^{-1} from 180 seconds onwards until the end of the experiment.

In the PXC IND CAF co-amorphous crystals appear to generate homogeneously throughout the entire structure and to grow progressively, promoting the generation of new crystals from the rubbery sample. Because of the elevated density of the crystals, it was not possible to accurately measure the length of the crystals and therefore the kinetics of crystal growth.

X-RAY DIFFRACTION

XRD was used to characterise the solid state of the initial materials, physical mixtures and co-amorphous systems by comparing the diffractograms to PDF-2 database entries (ICDD, 2008). Difractograms of the physical mixtures presented peaks belonging to each component of the mixture. This indicates that the grinding adopted to generate the physical mixtures did not alter the solid state of the components. Data was processed with the EVA analysis software for the quantification of the crystallinity of the systems, which revealed no traces of amorphous materials.

Analysis of the co-amorphous system has confirmed that the generated materials were amorphous confirming what observed in the DSC thermograms, characterised by a single glass transition and no melting points. The analysis with EVA confirmed that for each sample 100% of the material was in the amorphous state. The co-amorphous system of PXC IND and AC revealed a diffraction peak at 38^0 (2θ), therefore the sample was re-tested up to 60^0 (2θ) to evaluate the possible presence of crystalline materials of inorganic origin. Analysis revealed that the sample presented diffraction peaks typical of Aluminium, material from the vessel used to generate the co-amorphous systems.

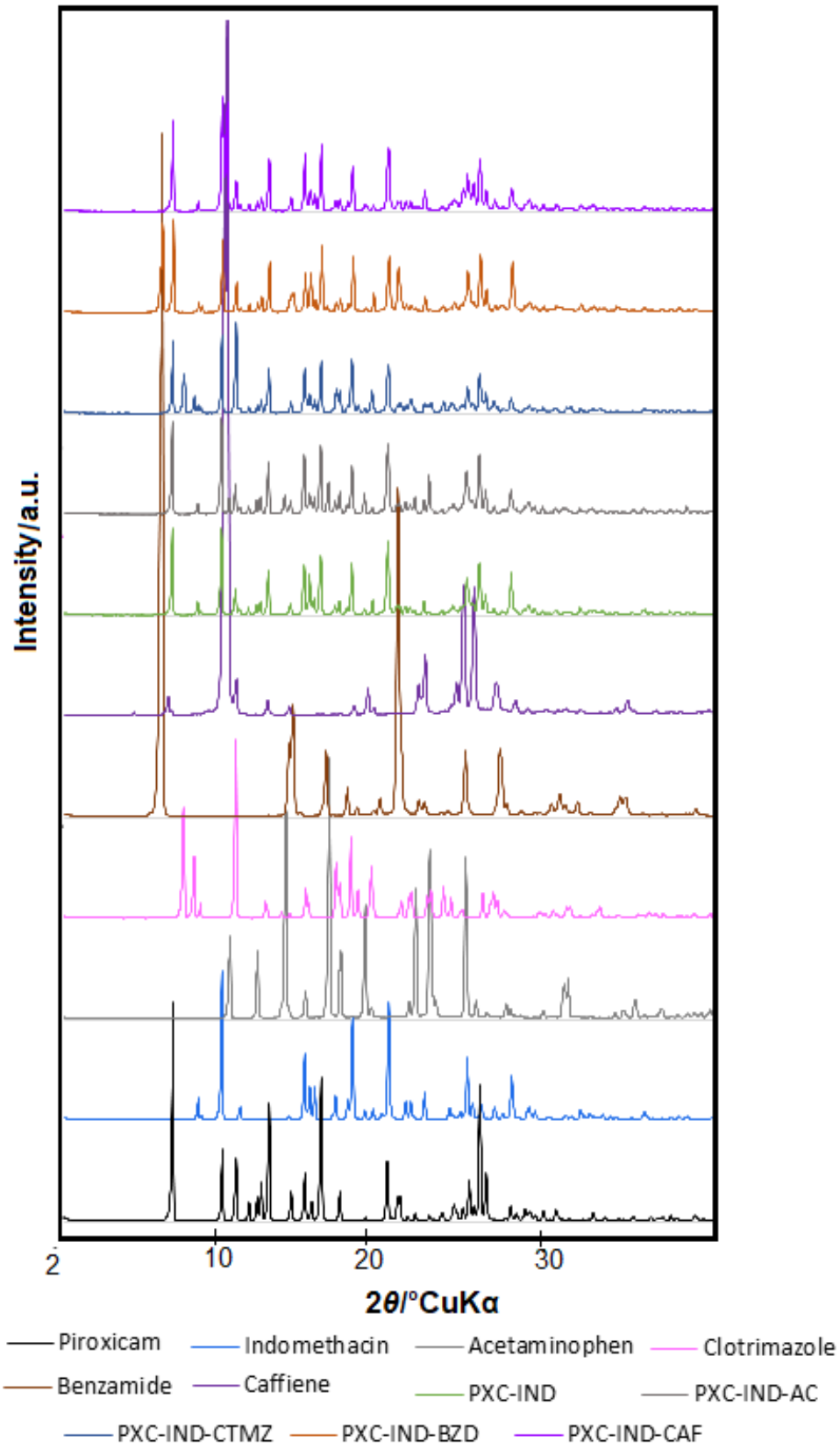

Figure 6 Overlay of diffractograms of pure chemicals and physical mixtures used to generate co-amorphous systems

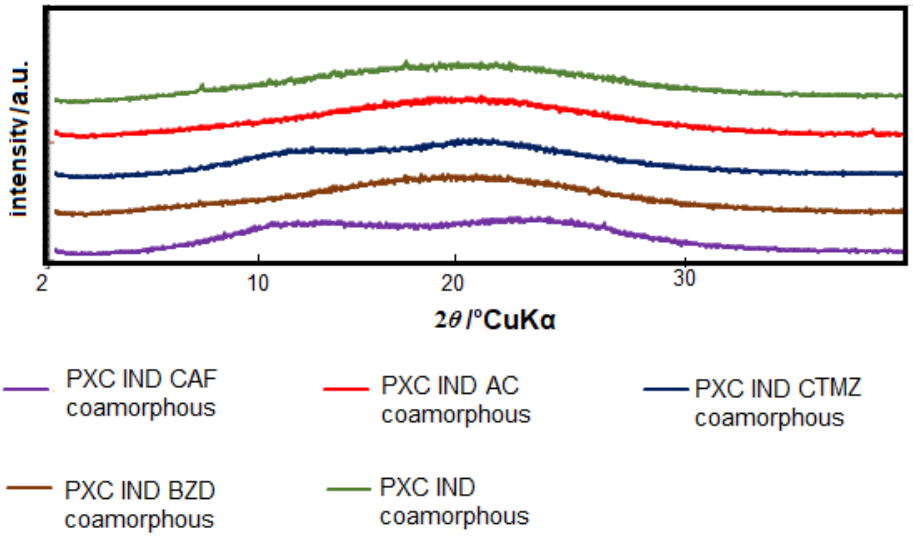

Figure 7 Overlay of diffraction traces of generated co-amorphous systems

Co-amorphous systems containing BZD and CAF kept isothermal for one hour at the starting temperature of the crystallisation were analysed with the same XRD methods used for the samples described above. Results for the PXC IND BZD allowed for the identification of the recrystallised material as PXC. The difractogram of the sample of co-amorphous PXC IND CAF after being held isothermal at the crystallisation temperature showed diffraction peaks that were not identified as belonging to the pure components or any of their known polymorphic forms. This suggests a number of possibilities including a polymorphic form of a single component or a co-crystal comprised of an unknown combination of at least two of the three starting materials. This is shown in Figure 8 where the crystalline material present in the mixture of PXC-IND-BZD clearly matches that of PXC whereas the diffactogram for PXC-IND-CAF does not.

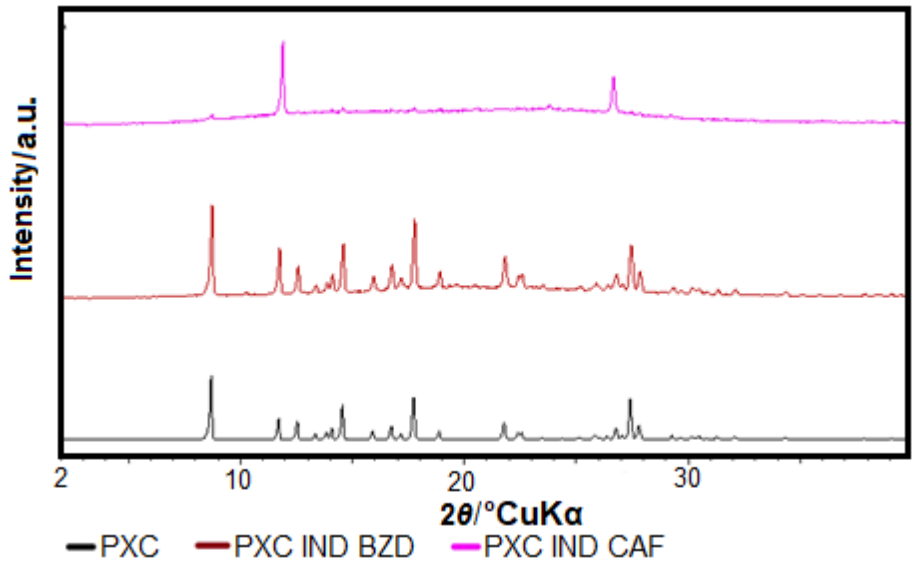

Figure 8 Overlay of diffraction traces of pure piroxicam (bottom), PXC-IND-BZD co-amorphous left isothermal for an hour at 100°C (middle) and XC-IND-CAF co-amorphous left isothermal for an hour at 183°C (top)

FOURIER TRANSFORM INFRA-RED SPECTROSCOPY

Infrared spectroscopy provides information on both the chemical and physical state, it was used to further characterise the solid state of pure compounds, physical mixtures and products. Molecular bonding vibrational frequencies are affected the molecular environment. When attempting to change the environment, such as changing the material from crystalline to amorphous, these frequencies will shift which can confirm successful modification of the environment.

Physical mixtures were characterised by bands relative to the crystalline components. The spectra of all tested physical mixtures were characterised by sharp bands typical of the crystalline state. Therefore, data indicates that in the physical mixtures the components were not interacting and that the grinding used to generate the dispersion did not influence the solid state of the adopted materials. The generated co-amorphous systems were characterised by broad bands, with absorbance's at the same wavelengths as the physical mixtures. This shows that no chemical interaction have occurred during the heating process and that the differences in peak shape are due to the change from crystalline to amorphous.

Broadening is typical of amorphous materials. Due to the lack of long range order a specific bond present, the amorphous material has numerous slightly different arrangements with neighbouring molecules, which shifts the vibrational frequency. Therefore, FT-IR results were in agreement with DSC and XRD data that indicates that the products of quench cooling were amorphous.

Band broadening has reduced significantly the band at 3338 cm^{-1} relative to the pyridin-2-yl-amino stretching of the piroxicam [27]. This band was present in all physical mixtures, but not visible in the co-amorphous systems. Two strong and resolute peaks at 1715 cm^{-1} and 1690 cm^{-1} relative to the C=O stretching of indomethacin and piroxicam were present in all physical mixtures. However, due to peak broadening of amorphous materials, these were merged in a single peak and shifted at 1680 cm^{-1}.

Another band shift recognised between crystalline and amorphous samples was relative to the C-H stretching which was measured at 2970 cm^{-1} in the crystalline samples and in the co-amorphous samples at 2980 cm^{-1}. Band shifting indicates that components of the studied co-amorphous systems were not only solid dispersions in amorphous phase, but also interacting. In PXC IND, PXC IND CAFF and PXC IND BZD systems, the intensity of this band was higher in the co-amorphous systems than in their crystalline counterparts.

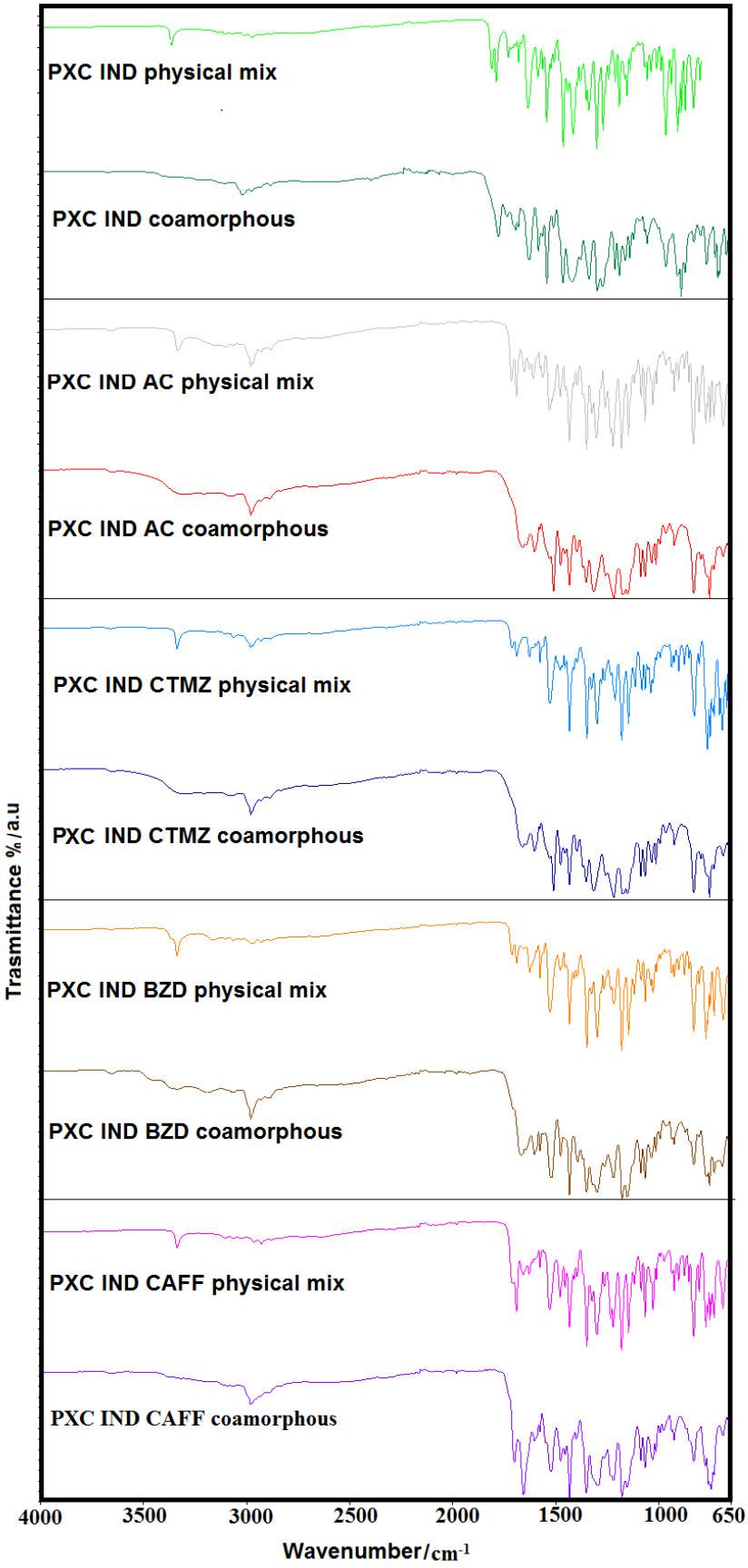

Figure 9 FT-IR overlay of pure chemicals, physical mixtures and generated co-amorphous systems

STABILITY

Over the 4 weeks' storage the binary co-amorphous system of PCX-IND has shown decrease in Tg (ΔTg) of 13.2^0C, which is significantly higher than the ΔTg of all the ternary co-amorphous under analysis. The decrease in Tg that occurred between the 3rd and the 4th week was significant for the binary system, whereas the ternary coamorphous appear to have a minimal ΔTg.

The PXC-IND-CTMZ was characterised by final ΔTg of 8.6^0C which was second only to that of the binary co-amorphous (Table 4). The systems that when freshly generated had the highest *Tg* in respect to the other co-amorphous, were instead characterised by the highest depression in *Tg* of all the stored samples. The other co-amorphous system, where all components had as pure compounds the tendency to form amorphous, PXC-IND-AC, shown instead a ΔTg of 5.0^0C. Results have shown that the addition to the amorphous PXC-IND of a third component with tendency to form crystalline material stabilises the system, causing a reduction of the ΔTg as shown in Table 5.

Table 4. Glass transition temperature of co-amorphous samples collected over 4 week period storage (*n=3*)

Systems	***Tg* fresh sample/°C**	***Tg* sample stored for 1 week/°C**	***Tg* sample stored for 2 weeks/°C**	***Tg* sample stored for 3 weeks/°C**	***Tg* sample stored for 4 weeks/°C**	**Δ*Tg* after 4 weeks/°C**
PXC-IND	57.6 ± 0.4	53.0 ± 2.6	52.0 ± 2.2	49.4 ± 1.9	44.4 ± 0.6	**13.2**
PXC-IND-BZD	31.0 ± 1.2	26.6 ± 0.3	26.1 ± 0.6	25.6 ± 0.7	27.3 ± 0.6	**3.7**
PXC-IND-CAF	45.8 ± 0.5	42.8 ± 0.9	42.0 ± 0.7	42.1 ± 0.4	42.4 ± 0.2	**2.1**
PXC-IND-AC	47.1 ± 1.3	42.5 ± 1.2	42.2 ± 1.4	43.5 ± 0.9	42.1 ± 1.6	**5.0**
PXC-IND-CTMZ	53.3 ± 1.2	48.7 ± 0.9	52.8 ± 2.1	46.3 ± 2.8	44.7 ± 2.1	**8.6**

CONCLUSIONS

Three component co-amorphous systems were reliably generated via a melt quench method. Components that have tendency to crystallise on cooling *i.e.* are not easily converted into amorphous phase, demonstrated not only the ability to form a co-amorphous system when combined into a co-amorphous mixture, but also showed greater stability of created co-amorphous system, with respect to the *Tg* values compared to compounds with tendency to create an amorphous material on rapid cooling. Short term stability, over four weeks, demonstrated that the ternary system is more stable when compared to the binary system. Unexpectedly it was found that the pure materials, which have a propensity to form crystalline materials on cooling, created more stable three-component systems with a much lower deviation in glass transition temperature across four weeks of storage. Based on this study it evident that the *Tg* of co-amorphous system can be altered using appropriate components of ternary mixture. The most commonly used physical parameters, *i.e. Tm* and *Tg*, may not be sufficient to predict the resulting *Tg* of the multicomponent co-amorphous systems. Therefore, knowledge of chemical interactions must be taken into account when manipulating *Tg* and selecting components for a ternary co-amorphous system.

Rapid cooling after melting is confirmed to be a valuable method for the amorphisation of single chemicals and in the generation of complex coamorphous systems. Improvement in stability of the ternary coamorphous systems in respect to binary coamorphous is valuable for the development of complex coamorphous, especially in the pharmaceutical field where coamorphous are used to improve apparent solubility and dissolution rate of active ingredients.

REFERENCES

1. Chavan RB, Thipparaboina R, Kumar D, Shastri NR. Co amorphous systems: A product development perspective. Int. J. Pharm. 2016;515(1):403-15.

2. Edueng K, Mahlin D, Bergström CAS. The Need for Restructuring the Disordered Science of Amorphous Drug Formulations. Pharm Res. 2017;34(9):1754-72.

3. Savjani KT, Gajjar AK, Savjani JK. Drug Solubility: Importance and Enhancement Techniques. ISRN Pharm. 2012:195727.

4. Sun Y, Zhu L, Wu T, Cai T, Gunn EM, Yu L. Stability of Amorphous Pharmaceutical Solids: Crystal Growth Mechanisms and Effect of Polymer Additives. AAPS J. 2012;14(3):380-8.

5. Hancock BC, Parks M. What is the True Solubility Advantage for Amorphous Pharmaceuticals? Pharm Res. 2000;17(4):397-404.

6. Graeser KA, Patterson JE, Zeitler JA, Rades T. The Role of Configurational Entropy in Amorphous Systems. Pharm. 2010;2(2):224-44.

7. Wang L-y, Zhu L, Sha Z-l, Li X-c, Wang Y-f, Yang L-b, et al. Characterization, thermal stability, and solid-state phase transition behaviors of gestodene polymorphs and amorphous phase. JTAC. 2017;127(2):1533-42.

8. Yu L. Amorphous pharmaceutical solids: preparation, characterization and stabilization. Adv. Drug Deliv. Rev. 2001;48(1):27-42.

9. Qian F, Huang J, Hussain MA. Drug–Polymer Solubility and Miscibility: Stability Consideration and Practical Challenges in Amorphous Solid Dispersion Development. J. Pharm. Sci. 2010;99(7):2941-7.

10. Karolewicz B, Gajda M, Pluta J, Górniak A. The effect of Pluronic F127 on the physicochemical properties and dissolution profile of lovastatin solid dispersions. JTAC. 2016;123(3):2283-90.

11. Yonemochi E, Sano S, Yoshihashi Y, Terada K. Diffusivity of amorphous drug in solid dispersion. JTAC. 2013;113(3):1505-10.

12. De Souza CMP, dos Santos JAB, do Nascimento AL, Chaves Júnior JV, de Lima Ramos Júnior FJ, de Lima Neto SA, et al. Thermal analysis study of solid dispersions hydrochlorothiazide. JTAC. 2018;131(1):681-9.

13. Rumondor ACF, Ivanisevic I, Bates S, Alonzo DE, Taylor LS. Evaluation of Drug-Polymer Miscibility in Amorphous Solid Dispersion Systems. Pharm. Res. 2009;26(11):2523-34.

14. Dametto PR, Dametto AC, Polese L, Ribeiro CA, Chorilli M, de Freitas O. Development and physicochemical characterization of solid dispersions containing praziquantel for the treatment of schistosomiasis. JTAC. 2017;127(2):1693-706.

15. Rumondor ACF, Stanford LA, Taylor LS. Effects of Polymer Type and Storage Relative Humidity on the Kinetics of Felodipine Crystallization from Amorphous Solid Dispersions. Pharm. Res. 2009a;26(12):2599.

16. Górska A, Szulc K, Ostrowska-Ligęza E, Bryś J, Wirkowska-Wojdyła M. Effect of composition and drying method on glass transition temperature, water sorption characteristics and surface morphology of newly designed β-lactoglobulin/retinyl palmitate/disaccharides systems. JTAC. 2017;130(1):177-85.

17. Yoshihashi Y, Iijima H, Yonemochi E, Terada K. Estimationof physical stability of amorphous solid dispersion using differential scanningcalorimetry. JTAC. 2006;85(3):689-92.

18. Guo Y, Shalaev E, Smith S. Physical stability of pharmaceutical formulations: solid-state characterization of amorphous dispersions. Tr. Anal. Chem. 2013;49:137–44.

19. Dengale SJ, Grohganz H, Rades T, Löbmann K. Recent advances in co-amorphous drug formulations. Adv. Drug Deliv. Rev. 2016;100:116-25.

20. Löbmann K, Grohganz H, Laitinen R, Strachan C, Rades T. Amino acids as co-amorphous stabilizers for poorly water soluble drugs – Part 1: Preparation, stability and dissolution enhancement. European Journal of Pharmaceutics and Biopharmaceutics. 2013;85(3, Part B):873-81.

21. Kaminska E, Adrjanowicz K, Zakowiecki D, Milanowski B, Tarnacka M, Hawelek L, et al. Enhancement of the Physical Stability of Amorphous Indomethacin by Mixing it with Octaacetylmaltose. Inter and Intra Molecular Studies. Pharmaceutical Research. 2014;31(10):2887-903.

22. Laitinen R, Löbmann K, Strachan CJ, Grohganz H, Rades T. Emerging trends in the stabilization of amorphous drugs. International Journal of Pharmaceutics. 2013a;453(1):65-79.

23. Yamamura S, Gotoh H, Sakamoto Y, Momose Y. Physicochemical properties of amorphous precipitates of cimetidine–indomethacin binary system. Eur. J. Pharm. Biopharm. 2000;49(3):259-65.

24. PubChem [Available from: https://pubchem.ncbi.nlm.nih.gov/. Accessed 20/11/2017.

25. Maheswaram MP, Mantheni D, Perera I, Venumuddala H, Riga A, Alexander K. Characterization of crystalline and amorphous content in pharmaceutical solids by dielectric thermal analysis. JTAC. 2013;111(3):1987-97.

26. Vrecer F, Vrbinc M, Meden A. Characterization of piroxicam crystal modifications. Int. J. Pharm. 2003;256(1–2):3-15.

27. Trivedi MK, Patil S, Shettigar H, Bairwa K, Jana S. Effect of Biofield Treatment on Spectral Properties of Paracetamol andPiroxicam. Chem Sci J. 2015;6(2).